

Parameter Estimation of Hodgkin-Huxley model of GnRH neurons

Dávid Cserecsik, Gábor Szederkényi, Katalin M. Hangos and Imre Farkas

Abstract—GnRH neurons are key elements of the reproductive neuroendocrine system and play important central regulating role in the dynamics of the hormonal cycle. A conductance-based Hodgkin-Huxley model structure is proposed in the form of nonlinear ordinary differential equations that is able to take into account upto- date biological literature data related to ion channels. The measurement data is originated from laboratory experiments done in the Institute of Experimental Medicine of the Hungarian Academy of Sciences and it includes whole cell patch-clamp recordings. The proposed neuron model is highly nonlinear in parameters and the evaluation of the objective function is computationally expensive, therefore the asynchronous parallel pattern search (APPS) procedure is used for identification which is a gradient-free optimization method. It can handle linear equality and inequality constraints and it has advantageous convergence properties [13]. The work is intended to be the first step in a bottom-up procedure which aims to build a hierarchical model of the GnRH pulse generator that includes the effects of ovarian hormones.

I. INTRODUCTION

Neurons are interesting dynamical systems where a combination of physico-chemical reactions and electrical phenomena are taking place. Dynamical modelling and parameter estimation of neurons is a challenging and quickly developing area with great importance in understanding the operation of certain physiological processes and potential use in therapy and drug design [15]. Although there were numerous attempts for the identification of neuron models (see, e.g. [27]), the computational methods and techniques in systems biology are not so well-developed and analyzed as in more traditional engineering fields [7].

The system of ovarian and pituitary hormones regulates and maintains the menstrual cycle in adult women. During the menstrual cycle, the anterior pituitary affected by Gonadotropine-releasing hormone (GnRH) secreted in the hypothalamus, secretes hormones in a pulsatile way to stimulate the growth and development of ovarian follicles: Follicle-stimulating hormone (FSH) and luteinizing hormone (LH). Consequently, cells in the ovaries secrete hormones which affect the secretion of GnRH and pituitary hormones: Estradiol (E_2), progesterone (P_4) and inhibin (Ih) [4].

Central control of reproduction in vertebrates is governed by a neuronal pulse generator that underlies the activity of hypothalamic neuroendocrine cells that secrete GnRH. Bursts

and prolonged episodes of repetitive action potentials have been associated with hormone secretion in this and other neuroendocrine systems.

The models of GnRH pulse generator, which can be found in literature nowadays, use generalized very simple neuron models and networks. Furthermore they are neither based on the known membrane properties of GnRH neurons, nor are able to describe the effect of ovary hormones [2], [9].

The main purpose of this work is to develop a method to estimate the parameters of a simple GnRH neuron model, based on laboratory measurements.

A. Hodgkin-Huxley type neural models

The Hodgkin-Huxley models are based on the pioneering work of A.L. Hodgkin and A.F. Huxley done in the 50's [12]. This fundamental concept in electrophysiology aims to describe the electrical activity of neural cells via two types of elements: the cell membrane is represented by a capacitance, and various ionic channels in the membrane are represented by voltage-dependent conductance elements. Each type of ionic current corresponds to conductance element with a certain Boltzmann-type voltage-conductance characteristic. In addition the change of the conductance-value is not instantaneous, but inhibits a first order linear dynamic, described by a time constant of which is also voltage dependent. The ions are driven through the voltage-dependent conductances by the ion-specific reversal potentials, which can be originated from different concentrations of various ions inside and outside the cell membrane.

II. THE GnRH NEURON

The pulsatile release of GnRH is driven by the intrinsic activity of GnRH neurons, which is characterized by bursts of action potentials correlated with oscillatory increases in intracellular Ca^{2+} .

Furthermore the dynamics of GnRH neurons is affected by peripheral hormones estradiol (E_2) [6], [22], [8], [10] and progesterone (P_4) [16], [3].

The morphological structure formed by the GnRH neurons and other neurons in the hypothalamus is called the GnRH pulse generator.

A. Basic membrane properties and ion channels of the GnRH neuron

In this subsection a chronological summary of some articles corresponding to the membrane properties of GnRH neurons is listed.

Experiments of Bosama et al. showed that the GT-1 cell line expressed a tetrodotoxin-sensitive Na channel, two types

This work was supported by the Hungarian Research Fund OTKA through grant K67625

D. Cserecsik, G. Szederkényi and K.M. Hangos are with the Process Control Research Group, Systems and Control Laboratory, Computer and Automation Research Institute, HAS, Budapest Hungary cserecsik@scl.sztaki.hu

I. Farkas is with the Department of Endocrine Neurobiology, Institute of Experimental Medicine, HAS, Budapest, Hungary

of Ca channels, three types of outward K channels and a K inward rectifier [1].

Kusano et al. identified an inward rectifier type current, a tetrodotoxin-sensitive Na^+ current (I_{Na}) and two major types of K^+ currents, a transient current (I_A), a delayed rectifier current (I_K) and low- and high-voltage activated Ca^{2+} currents in cultures of embryonic GnRH neurons [21].

The families of electrotonic potentials evoked in individual adult GnRH neurons in response to short (20-30 msec duration) and long (200 msec) duration intracellular current pulses were found to be heterogeneous [24]. The most striking difference was observed in response to 200 msec hyperpolarizing current pulses where four main profiles (types I-IV) were consistently observed.

Adult GnRH neurons were found to fire Na^+ dependent action potentials, because 0.5 μ mol TTX abolished evoked action potentials in all cells tested.

These investigations [24] point to the probability of presence of $I_{Q/H}$ (large current potassium-activated) I_A (rapidly inactivating) and I_K (delayed rectifier) potassium channels.

According to [11], GnRH neurons express a variety of sodium, type I_{IR} (inward rectifying), I_A , and $I_{Q/H}$ potassium. and type T and N Ca^{2+} channels.

Constantin et al. found that Whole-cell recordings of voltage-gated outward K^+ currents in GT1-1 neurons revealed at least two different components of the current. These included a rapidly activating transient component and a more slowly activating, sustained component [5]. Furthermore, according to this article, GT1-1 cells also express inwardly rectifying K^+ currents ($I_{K(IR)}$) that were activated by hyperpolarization in the presence of elevated extracellular K^+ . These results of this article also indicate that specific subtypes of K^+ channels in GT1-1 cells can have distinct roles in the amplitude modulation or frequency modulation of Ca^{2+} signaling.

III. MATERIALS AND METHODS

Based on literature data about the ion channels of the GnRH neuron and properties of ion channels, a simple GnRH neuron-model can be developed and identified via further literature data and voltage-clamp measurements.

This basic membrane dynamics-model is considered to be appropriate, if it approximates available measurement data quantitatively good.

Thereafter, the model can be extended to take the complex effects of estradiol on the dynamics of membrane potential into account.

A. Measurement data

The mouse was decapitated, and the brain was rapidly removed and placed in ice-cold temperature. Brains were blocked and glued to the chilled stage of a vibratome, and 150- μ m-thick coronal slices containing the medial septum through to the preoptic area were prepared. The slices were then incubated at 30°C for 30 min in oxygenated recording ACSF (rACSF) consisting of (in mM): 118 NaCl, 3 KCl, 2.5 CaCl₂, 1.2 MgCl₂, 11 D-glucose, 10 HEPES, and 25

NaHCO₃, pH 7.3, and thereafter kept at room temperature (20-23°C) for at least 1 hr before recording.

1) *Whole-cell recording of GnRH neurons:* Slices were transferred to the recording chamber, held submerged, and continuously superfused with oxygenized extracellular fluid. In order to record the neurons, the equilibrated hemi-slices were placed in an immersion-type recording chamber. All recordings were made at room temperature (20 - 23°C).

In order to visualize GnRH neurons in the brain slices, GnRH-enhanced green fluorescent protein (GnRH-GFP) transgenic mice (kind gift by Dr. Suzanne Moenter) were chosen in which the GnRH promoter drives selective GFP expression in the majority of GnRH neurons.

B. Model development

1) *The suggested model framework of single cell models:* A single compartment Hodgkin-Huxley (HH) type model is suggested, which can be extended to a multicompartmental structure, if needed for the description of bursting. The main benefits of this model class are the following:

- Modularity: Each ion channel is represented by an element of the model (conductance), so different ion channels can be taken into account separately, and in a modular way. This way ensures the integration of the most available literature data into the model.
- The properties of specific ion channels can be measured separately via voltage clamp (reveral potential-based) methods, and pharmacological (TTX, TEA, etc. based) methods. These types of measurements can gather data corresponding to specific elements of the model. This implies the benefit of the opportunity, that various elements of the model can be identified separately, using different parameter estimation methods, if needed.
- Because the different ion channels are described by different elements of the model, the model is capable to be extended with equations describing the effect of estradiol, acting on specific ion channels.

Elements of the model: According to the literature data detailed in II-A, previous results point to the existence of the following components on the level of conductance elements in the HH model:

- Na^+ channel: A simple voltage gated inward rectifier Na^+ channel can be assumed, with standard characteristics [1], [21]. The current related to this channel will be denoted with I_{Na1} .
- A voltage gated transient or rapidly activating/inactivating K^+ channel is taken into account, responsible for the rapid, transient component of the outward K^+ current (I_{K1}) [21], [5], [24], [1], [11].
- A voltage gated delayed outward rectifier K^+ channel can be assumed, which contributes to the more slowly activating, sustained component of the outward K^+ current (I_{K2}) [21], [5], [24], [1], [11].
- static leakage currents with constant conductance (I_L).

These types of conductances can be taken into account as building blocks, which can be used to find minimal models

of observed characteristic behaviors of GnRH neurons [24], [11].

The **equivalent electric circuit** of a one-compartment GnRH neuron model in the case when all conductances are taken into account is depicted as in fig. 1

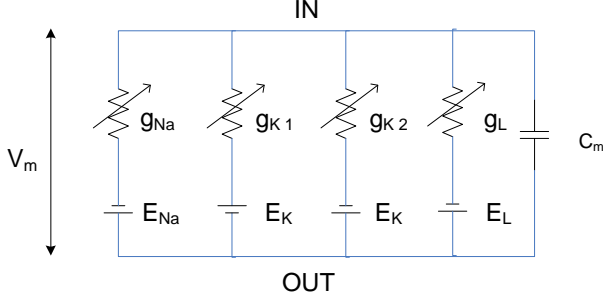


Fig. 1. Parallel conductance model, with conductances representing different ion channels

Literature data of qualitative features and parameters related to some of the various detailed ion channels can be found in [23], [26], [17]. The remaining parameters can be objects to further literature research, and experiments, if necessary.

Model equations: The model depicted in fig. 1 can be described with the following equations:

$$\dot{V} = -\frac{(I_{Na} + I_{K1} + I_{K2} + I_L)}{C} + \frac{1}{C}I_{ex} \quad (1)$$

$$\dot{h}_1 = (h_{1\infty}(V) - h_1)/\tau_{h1}(V) \quad (2)$$

$$\dot{m}_2 = (m_{2\infty}(V) - m_2)/\tau_{m2}(V) \quad (3)$$

$$\dot{h}_2 = (h_{2\infty}(V) - h_2)/\tau_{h2}(V) \quad (4)$$

$$\dot{m}_3 = (m_{3\infty}(V) - m_3)/\tau_{m3}(V) \quad (5)$$

$$\dot{h}_3 = (h_{3\infty}(V) - h_3)/\tau_{h3}(V) \quad (6)$$

where the currents of the ion channels are given by

$$I_{Na} = \bar{g}_{Na} m_1 m_{1\infty}(V) h_1 (V - E_{Na}) \quad (7)$$

$$I_{K1} = \bar{g}_{K1} m_2^4 h_2 (V - E_K) \quad (8)$$

$$I_{K2} = \bar{g}_{K2} m_3 h_3 (V - E_K) \quad (9)$$

and the so-called leakage current is

$$I_L = \bar{g}_L (V - E_L). \quad (10)$$

The exciting current I_{ex} in (1) can be computed from the exciting voltage V_{ex} (which is the real physical input) as

$$I_{ex} = p \cdot (V_{ex} - V), \quad (11)$$

where p is a known constant parameter.

The E_{Na} , E_K and E_{Ca} parameters in eqs. (7)-(9) are the reversal potentials of the corresponding ions, and the $m_{i\infty}$, $h_{i\infty}$ and τ notations are defined as nonlinear Boltz-

mann and Gauss functions:

$$m_{i\infty}(V) = \left(1 + e^{\frac{V_{h_{i1}} - V}{K_{i1}}}\right)^{-1}, \quad i = 1, 2, 3 \quad (12)$$

$$h_{i\infty}(V) = \left(1 + e^{\frac{V_{h_{i2}} - V}{K_{i2}}}\right)^{-1}, \quad i = 1, 2, 3 \quad (13)$$

$$\tau_{mi}(V) = C_{b_{i1}} + C_{a_{i1}} e^{\frac{-(V_{m_{i1}} - V)^2}{\sigma_{i1}^2}}, \quad i = 2, 3 \quad (14)$$

$$\tau_{h1}(V) = C_{a_{12}} e^{\frac{V_{m_{12}} - V}{\sigma_{12}}} \quad (15)$$

$$\tau_{hi}(V) = C_{b_{i2}} + C_{a_{i2}} e^{\frac{-(V_{m_{i2}} - V)^2}{\sigma_{i2}^2}}, \quad i = 2, 3 \quad (16)$$

The parameters of the Boltzmann and Gauss functions ($V_{h_{i1,2}}$, $K_{i1,2}$, $C_{b_{i1,2}}$, $C_{a_{i1,2}}$, $V_{m_{i1,2}}$ and $\sigma_{i1,2}$), and the E_{Na} , E_K and E_{Ca} reversal potential values were determined using literature data [15], [26], and measurement data corresponding to the intra- and extracellular fluid concentrations.

C. Parameter estimation

1) *Basic identification setup:* The manipulated external input to the system was the excitation voltage V_{ex} . Three square signals of different amplitudes shown in fig. 2 were used as inputs. The measured output was the total output membrane current:

$$I_{out} = I_{Na} + I_{K1} + I_{K2} + I_L$$

The measured outputs for the corresponding input voltages can be seen in fig. 3. The sampling time of the measurements was 0.1 ms.

The known parameter values (taken from literature and obtained from previous measurements) were the following:

$$V_{h_{11}} = -30, V_{h_{21}} = -60, V_{h_{31}} = -3 \quad (17)$$

$$K_{11} = 5.5, K_{21} = 8.5, K_{31} = 10 \quad (18)$$

$$V_{h_{12}} = -70, V_{h_{22}} = -78, V_{h_{32}} = -51 \quad (19)$$

$$K_{12} = -5.8, K_{22} = -6, K_{32} = -12 \quad (20)$$

$$V_{m_{12}} = -40, V_{m_{21}} = -58, V_{m_{31}} = -50 \quad (21)$$

$$\sigma_{12} = 33, \sigma_{21} = 25, \sigma_{31} = 30 \quad (22)$$

$$C_{a_{21}} = 2, C_{a_{31}} = 47, C_{b_{21}} = 0.37, C_{b_{31}} = 5 \quad (23)$$

$$V_{m_{22}} = -78, V_{m_{32}} = -50, \sigma_{22} = 25, \sigma_{32} = 50 \quad (24)$$

$$C_{a_{22}} = 45, C_{a_{32}} = 1000, C_{b_{22}} = 19, C_{b_{32}} = 360 \quad (25)$$

$$E_{Na} = 70, E_K = -90, E_{Ca} = 140, E_L = -50 \quad (26)$$

The estimated parameters were the membrane capacitance C in (1) and the \bar{g}_{Na} , \bar{g}_{K1} , \bar{g}_{K2} , \bar{g}_L conductances in eqs (7)-(10).

The objective function of the estimation was the standard two-norm of the difference between the measured and computed output currents for the three measurements, i.e.

$$V(\theta) = \frac{1}{N_1} \|I_{out,1}^m - I_{out,1}^s\|_2 + \frac{1}{N_2} \|I_{out,2}^m - I_{out,2}^s\|_2 + \frac{1}{N_3} \|I_{out,3}^m - I_{out,3}^s\|_2 \quad (27)$$

where θ is the estimated parameter vector, and $I_{out,i}^m$ and $I_{out,i}^s$ for $i = 1, 2, 3$ denote the measured and model

computed (simulated) total output current (as a discrete time sequence) for the i th measurement, respectively. Furthermore, N_i is the number of data points in the case of the i th measurement.

D. Optimization algorithm

Since none of the state variables in eqs. (1)-(6) were measured, a simulation based minimization of the objective function was performed. Because of the model nonlinearity, the objective function value can be a complicated function of the estimated parameters. Moreover, the precise simulation of the system dynamics for a given parameter set is computationally quite demanding, i.e. a few hundred evaluations of the objective function takes a couple of hours on a typical desktop PC. This also means that avoiding the numerical approximation of the gradients of the objective function was desirable in our case.

The above facts motivated us to choose the freely available Asynchronous Parallel Pattern Search (APPS) algorithm for parameter estimation. Parallel pattern search (PPS) is a useful tool for derivative-free optimization where the number of variables is not large (about fifty or less) and the objective function is expensive to evaluate [14]. The basic PPS algorithm is very simple, its main steps are the following (where f denotes the objective function to be minimized):

Initialization:

- Set the iteration counter $k = 0$.
- Select a set of search directions $\mathcal{D} = \{d_1, \dots, d_p\}$.
- Select a step-length control parameter Δ_0 .
- Select a stopping tolerance tol .
- Select a starting point x_0 and evaluate $f(x_0)$.

Iteration:

- 1) Compute $x_k + \Delta_k d_i$ and evaluate $f(x_k + \Delta_k d_i)$, for $i = 1, \dots, p$ concurrently.
- 2) Determine x_+ and $f(x_+)$ such that $f(x_+) = \min\{f(x_k + \Delta_k d_i), i = 1, \dots, p\}$.
- 3) If $f(x_+) < f(x_k)$, then $x_k \leftarrow x_+$ and $f(x_k) \leftarrow f(x_+)$. Else $\Delta_k \leftarrow \frac{1}{2} \Delta_k$.
- 4) If $\Delta_k > tol$, $k \leftarrow k + 1$, go to Step 1. Else, exit.

The APPS algorithm is an asynchronous extension of the PPS method that efficiently handles situations when the individual objective function evaluations may take significantly different time intervals and therefore it is very suitable to be implemented in a parallel or grid environment. Furthermore, recent implementations of the APPS method handle bound and linear constraints on the parameters [18]. The global convergence of APPS under standard assumptions is also proved [19]. These advantageous properties suggest that APPS can be a good choice to solve simulation-intensive optimization problems.

IV. RESULTS AND DISCUSSION

The approximate order of magnitude of the estimated parameters was known from literature data, therefore an acceptable initial guess could be made for them. The parameters were scaled appropriately during the optimization to

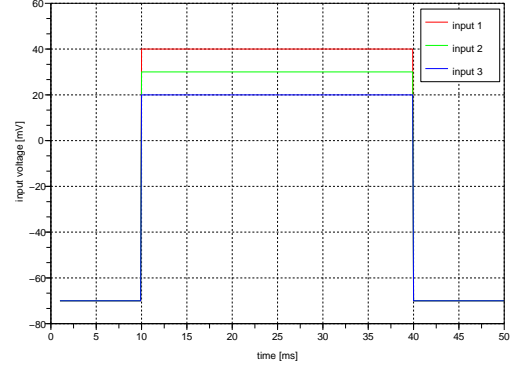


Fig. 2. Input voltages applied to the system

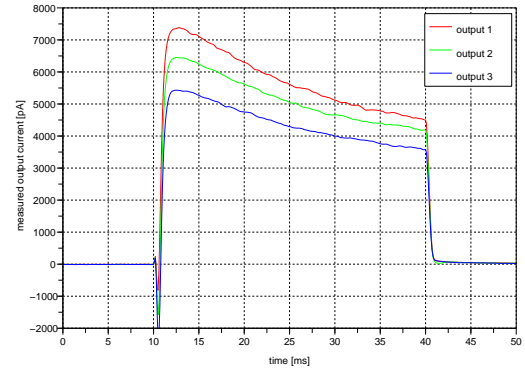


Fig. 3. Measured output total membrane currents

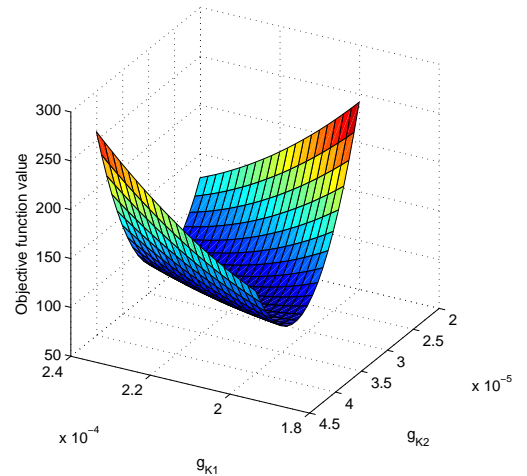


Fig. 4. Dependence of the objective function on g_{K1} and g_{K2}

transform each value into the $[0 \ 1]$ interval. The simulations were compared to three different cases of voltage clamp measurements' data series. In the first case, the parameters

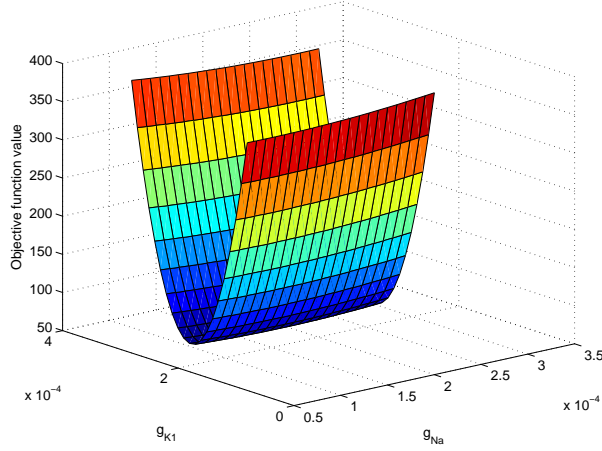


Fig. 5. Dependence of the objective function on g_{Na} and g_{K1}

of the voltage step were -70 and 40 mV, and it was applied between 10 and 40 ms. Multiple runs of the APPS algorithm were performed starting from different initial conditions within the physically acceptable domain. The method converged well for each run and produced acceptable final results in the same order of magnitude with very similar objective function value. A typical result from these experiments is the following. The algorithm needed 255 function evaluations altogether and provided the model parameters with the objective function value $V(\theta^*) = 63.91$:

$$C = 4.134 nF, \quad \bar{g}_{Na} = 2.253 \cdot 10^{-4} mS, \quad (28)$$

$$\bar{g}_{K1} = 2.079 \cdot 10^{-4} mS, \quad \bar{g}_{K2} = 2.279 \cdot 10^{-5} mS, \quad (29)$$

$$\bar{g}_L = 9.046 \cdot 10^{-6} mS \quad (30)$$

Results of the voltage steps are depicted in figure 6.

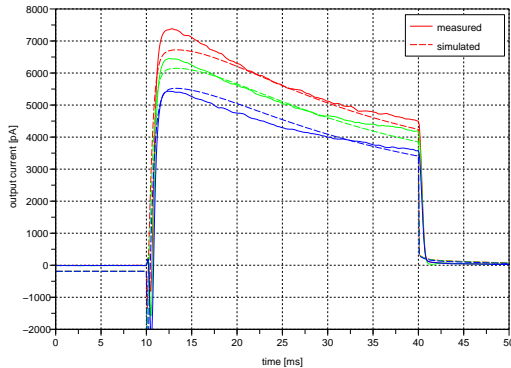


Fig. 6. Simulated and measured total membrane currents

As it can be seen from figures 4 and 5, the sensitivity of the objective function to various parameters differs in an order of magnitude. Fig. 5 shows that the loss function depends heavily on the maximum conductance of the 1st

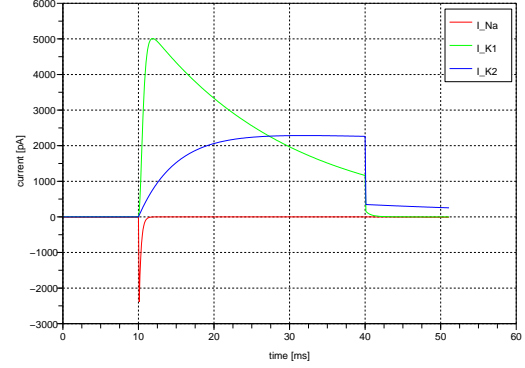


Fig. 7. Simulated sodium and potassium currents

potassium channel, but hardly on the maximum conductance of the sodium channel.

This can be related also to the measurement method: in the case of voltage-clamp measurements, the sodium current for example influences only the negative spike at the beginning of the voltage step so it hardly affects the objective function.

In addition, while the Hodgkin-Huxley type models exhibit several benefits (for example strong physical basis, and modularity, which probably will hold great values in the case of future measurements with specific channel-blockers), it seems that the weak identifiability and correlation between model parameters appear among his drawbacks.

Furthermore the sensitivity to a specified parameter strongly depends on the values of the other parameters. Anyway the resulting parameters are in a physiologically feasible region, and can serve as starting point for further estimation procedures. Furthermore, it can be noted that the fitting of the response function is not perfect (especially in the region of the local maxima), as it can be seen in figure 6. This implies the re-consideration of parameters, that were determined from literature data (parameters of the sigmoid and Gauss-functions etc.), and even the qualitative features of the model (for example the lack of activation dynamics in the case of sodium current).

As it can be clearly seen in figure 7, the two potassium currents are qualitatively different: I_{K1} is a transient-type current with an early maxima, and I_{K2} is monotone, slower current.

V. CONCLUSIONS AND FUTURE WORK

In this work a Hodgkin-Huxley type model of the GnRH neuron was suggested, based on biological literature data. Based on voltage-clamp measurements, the asynchronous parallel pattern search (APPS) procedure was used for parameter identification.

A. Future work

The main aim of the work is to create a simple model of the GnRH neuron, which can describe the characteristic qualitative features of this class of neurons related to

basic electrophysiological properties, and interactions with the ovarian elements of the neuroendocrine reproductive cycle. Obviously, the next stage in the identification process requires the application of further measurement data, corresponding to current clamp measurements, and measurements with the application of various selective ion-channel blocking agents (TEa, TTX etc). Based on further measurement data, the model will be re-adjusted, and extended, if necessary with further ionic currents. One of the future tasks will be to theoretically analyze the identifiability of the model.

REFERENCES

- [1] M.M. Bosama. Ion channel properties and episodic activity in isolated immortalized gonadotropin-releasing hormone (GnRH) neurons. *Journal of Membrane Biology*, 136:85–96, 1993.
- [2] D. Brown, A.E. Herbison, J.E. Robinson, R.W. Marrs, and G. Leng. Modelling the lutenizing hormone-releasing hormone pulse generator. *Neuroscience*, 63:869–879, 1994.
- [3] N. Chabbert-Buffet, D.C. Skinnerb, A. Caratyb, and P. Boucharda. Neuroendocrine effects of progesterone. *Steroids*, 65:613–620, 2000.
- [4] P.M. Conn and M.E. Freeman. *Neuroendocrinology in Physiology and Medicine*. Humana Press, 999 Riverview Drive Suite 208 Totowa New Jersey 07512, 2000.
- [5] J.L. Constantin and A.C. Charles. Modulation of Ca^{2+} signaling by K^+ channels in a hypothalamic neuronal cell line (GT-1). *Journal of Neurophysiology*, 85:295–304, 2001.
- [6] R.A. DeFazio and S.M. Moenter. Estradiol feedback alters potassium currents and firing properties of gonadotropin-releasing hormone neurons. *Molecular Endocrinology*, 16:2255–2265, 2002.
- [7] P. Dhurjati and R. Mahadevan. Systems biology: the synergetic interplay between biology and mathematics. *the canadian journal of Engineering*, 86:141, 2008.
- [8] I. Farkas, P. Varju, and Zs. Liposits. Estrogen modulates potassium currents and expression of the Kv4.2 subunit in GT1-7 cells. *Neurochemistry International*, 50:619–627, 2007.
- [9] J.D. Gordan, B.J. Attardi, and D.W. Pfaff. Mathematical exploration of pulsatility in cultured gonadotropin-releasing hormone neurons. *Neuroendocrinology*, 67:2–17, 1998.
- [10] A.E. Herbison. Estrogen positive feedback to gonadotropin-releasing hormone (GnRH) neurons in the rodent: The case for the rostral periventricular area of the third ventricle (RP3V). *Brain Research Reviews*, doi:10.1016/j.brainresrev.2007.05.006, 2007.
- [11] A.E. Herbison, J.R. Pape, S.X. Simonian, M.J. Skynner, and J.A. Sim. Molecular and cellular properties of GnRH neurons revealed through transgenics in mouse. *Molecular and Cellular Endocrinology*, 185:185–194, 2001.
- [12] A.L. Hodgkin and A.F. Huxley. A quantitative description of membrane current and application to conduction and excitation in nerve. *Journal of Physiology*, 117:500–544, 1952.
- [13] P. Hough, T. Kolda, and V. Torczon. Asynchronous parallel pattern search for nonlinear optimization. *SIAM Journal of Scientific Computing*, 23:134–156, 2002.
- [14] P. D. Hough, T. G. Kolda, and V. J. Torczon. Asynchronous parallel pattern search for nonlinear optimization. *SIAM Journal on Scientific Computing*, 23:134–156, 2000.
- [15] E.M. Izhikevich. *Dynamical Systems in Neuroscience*. The MIT Press, 999 Riverview Drive Suite 208 Totowa New Jersey 07512, 2005.
- [16] F.J. Karsch, J.T. Cummins, G.B. Thomas, and I.J. Clarke. Steroid feedback inhibition of pulsatile secretion of gonadotropin-releasing hormone in the ewe. *Biology of Reproduction*, 36:1207–18, 1987.
- [17] M. Kato, K. Ui-Tei, M. Watanabe, and Y. Sakuma. Characterization of voltage-gated calcium currents in gonadotropin-releasing hormone neurons tagged with green fluorescent protein in rats. *Endocrinology*, 144:5118–5125, 2003.
- [18] T. G. Kolda. Revisiting asynchronous parallel pattern search for nonlinear optimization. *SIAM J. Optim.*, 16:563–586, 2005.
- [19] T.G. Kolda and V.J. Torczon. On the convergence of asynchronous parallel pattern search. *SIAM J. Optim.*, 14:939–964, 2004.
- [20] L.Z. Krsmanovic, S.S. Stojilkovic, F. Merelli, S.M. Dufour, M.A. Virmani, and K.J. Catt. Calcium signaling and episodic secretion of gonadotropin-releasing hormone in hypothalamic neurons. *Proceedings of the National Academy of Sciences of the USA*, 89:8462–8466, 1992.
- [21] K. Kusano, S. Fueshko, H. Gainer, and S. Wray. Electrical and synaptic properties of embryonic lutenizing hormone-releasing hormone neurons in explant cultures. *Proceedings of the National Academy of Sciences of the USA*, 92:3918–3992, 1995.
- [22] R.A. Maurer, K.E. Kim, W.E. Schoderbek, M.S. Robertson, and D.J. Glenn. Regulation of glycoprotein hormone alpha-subunit gene expression. *Recent Progress in Hormone Research*, 129:1175–82, 1999.
- [23] H. Rehm and B.L. Tempel. Voltage-gated k^+ channels of the mammalian brain. *FASEB J.*, 5:164–170, 1991.
- [24] J.A. Sim, M.J. Skynner, and A.E. Herbison. Heterogeneity in the basic membrane properties of postnatal gonadotropin-releasing hormone neurons in the mouse. *The Journal of Neuroscience*, 21:1067–1075, 2001.
- [25] S.S. Stojilkovic, L.Z. Krsmanovic, D.J. Spergel, and K.J. Catt. GnRH neurons: intrinsic pulsatility and receptor-mediated regulation. *Trends in Endocrinology and Metabolism*, 5:201–209, 1994.
- [26] K. Talavera and B. Nilius. Biophysics and structure-function relationship of T-type Ca^{2+} channels. *Cell Calcium*, 40:97–114, 2006.
- [27] J.H. Tien and J. Guckenheimer. Parameter estimation for bursting neural models. *Journal of Computational Neuroscience*, 24:358–373, 2008.